Research article

NMR IN BIOMEDICINE

Received: 4 February 2013, Revised: 6 May 2013, Accepted: 16 May 2013, Published online in Wiley Online Library: 20 June 2013

(wileyonlinelibrary.com) DOI: 10.1002/nbm.2987

MR elastography in a murine stroke model reveals correlation of macroscopic viscoelastic properties of the brain with neuronal density

Florian Baptist Freimann[a], Susanne Müller[b], Kaspar-Josche Streitberger[c], Jing Guo[c], Sergej Rot[a], Adnan Ghori[a], Peter Vajkoczy[a], Rolf Reiter[c], Ingolf Sack[c]* and Jürgen Braun[d]*

The aim of this study was to investigate the influence of neuronal density on viscoelastic parameters of living brain tissue after ischemic infarction in the mouse using MR elastography (MRE). Transient middle cerebral artery occlusion (MCAO) in the left hemisphere was induced in 20 mice. *In vivo* 7-T MRE at a vibration frequency of 900 Hz was performed on days 3, 7, 14 and 28 ($n = 5$ per group) after MCAO, followed by the analysis of histological markers, such as neuron counts (NeuN). MCAO led to a significant reduction in the storage modulus in the left hemisphere relative to contralateral values ($p = 0.03$) without changes over time. A correlation between storage modulus and NeuN in both hemispheres was observed, with correlation coefficients of $R = 0.648$ ($p = 0.002$, left) and $R = 0.622$ ($p = 0.003$, right). The loss modulus was less sensitive to MCAO, but correlated with NeuN in the left hemisphere ($R = 0.764$, $p = 0.0001$). In agreement with the literature, these results suggest that the shear modulus in the brain is reduced after transient ischemic insult. Furthermore, our study provides evidence that the *in vivo* shear modulus of brain tissue correlates with neuronal density. In diagnostic applications, MRE may thus have diagnostic potential as a tool for image-based quantification of neurodegenerative processes. Copyright © 2013 John Wiley & Sons, Ltd.

Keywords: MR elastography; mouse brain; stroke; ischemia; middle cerebral artery occlusion; neuronal density; viscoelastic network

INTRODUCTION

The interruption of blood flow in a cerebral artery causes brain ischemia with a dramatic impact on brain metabolism and function. The pathogenesis of stroke and tissue repair after stroke involve multiple transient events and permanent reorganization processes, including vascular dilatation, neovascularization, inflammation, neuronal decline and gliosis (1–4). At autopsy, stroke areas are recognized as being softer than surrounding tissue or, conversely, present with higher stiffness when stroke repair with scar formation has occurred. As such, the viscoelastic properties of the brain provide biomarkers which are sensitive to the inherent mechanical constitution of cerebral parenchyma, and which change significantly in response to the disruption of cerebral blood flow and the following cascade of tissue degradation and regeneration processes (5,6).

In a recent study by Martín *et al*. (6), the tissue's mechanical response to an altered vessel size and vascularization after middle cerebral artery occlusion (MCAO) in rats was analyzed by ultrasound shear wave imaging (SWI) (7). The authors observed tissue softening in the hemisphere affected by stroke 1 day after the injury, suggesting the sensitivity of the brain's mechanical properties to the loss of structural organization by ischemic infarction. The authors of this study also observed bilateral angiogenesis in response to transient MCAO, whereas the decline in elasticity was measured by SWI only in the hemisphere containing the ischemic lesion.

An alternative method of elasticity imaging in small animal brains is MR elastography (MRE) (8–12). Recent studies have shown that demyelination and inflammation reduce the elasticity of brain

* *Correspondence to: J. Braun, Institute of Medical Informatics, Charité — Universitätsmedizin Berlin, Hindenburgdamm 30, 12200 Berlin, Germany.*
E-mail: juergen.braun@charite.de
I. Sack, Department of Radiology, Charité – Universitätsmedizin Berlin, Charitéplatz 1, 10117 Berlin, Germany.
E-mail: ingolf.sack@charite.de

a *F. B. Freimann, S. Rot, A. Ghori, P. Vajkoczy*
Department of Neurosurgery, Charité – Universitätsmedizin Berlin, Berlin, Germany

b *S. Müller*
Center for Stroke Research Berlin, Charité – Universitätsmedizin Berlin, Berlin, Germany

c *K.-J. Streitberger, J. Guo, R. Reiter, I. Sack*
Department of Radiology, Charité – Universitätsmedizin Berlin, Berlin, Germany

d *J. Braun*
Institute of Medical Informatics, Charité – Universitätsmedizin Berlin, Berlin, Germany

Abbreviations used: *AD, Alzheimer's disease; ANOVA, analysis of variance; FLASH, fast low-angle shot; FOV, field of view; GFAP, glial fibrillary acidic protein; MCAO, middle cerebral artery occlusion; MRE, MR elastography; MS, multiple sclerosis; MSG, motion-sensitizing gradient; NeuN, neuron count; NPH, normal pressure hydrocephalus; ROI, region of interest; SWI, ultrasound shear wave imaging.*

NMR IN BIOMEDICINE

tissue (13,14). Unlike SWI, MRE is capable of measuring viscoelastic constants in the human brain without interventions (15–17). In a variety of experimental pilot studies, cerebral MRE was used to measure the viscoelastic properties in healthy volunteers (18–22), and in patients with multiple sclerosis (MS) (23,24), Alzheimer's disease (AD) (25), brain tumors (26) and normal pressure hydrocephalus (NPH) (27,28), or to reveal pressure-related properties (29,30) or anisotropic elastic constants (31) of the healthy brain. From these pilot studies, we have learnt that different physiological events and various neurological disorders are accompanied by widespread softening of the cerebral parenchyma, suggesting that the brain's viscoelastic properties may reflect fundamental patterns of neuronal integrity.

To further unravel the relationship between microstructure and macromechanical properties of the brain, we used an MCAO mouse model to alter the structural organization of brain tissue and to correlate mechanical properties with histological parameters. Specifically, we measured the complex shear modulus of the brain at a harmonic vibration frequency of 900 Hz, which represents both storage and loss properties by its real part G' and imaginary part G'', respectively. Histologically, we quantified the neuron count (NeuN), the number of glial fibrillary acidic proteins (GFAPs) and markers of apoptosis. GFAP allows the visualization of astrocytes, in particular reactive astrocytes and glial scar formation. To account for time effects, all parameters were measured repeatedly on different days after MCAO.

Based on our experience with MRE in patients (23,24,27,28), we hypothesized that neurodegeneration and the loss of neurons associated with stroke would reduce brain stiffness. Although studies on single neurons, tissue samples (32) and demyelinated axons (13) have suggested that brain stiffness correlates with neuronal integrity, no direct correlation of the macroscopic mechanical properties of *in vivo* brain with NeuN has been reported. Therefore, our study aims to determine the sensitivity of cerebral MRE for the diagnosis of disseminated structural disintegration and neuronal loss in cerebral tissue associated with multiple neurological disorders.

MATERIALS AND METHODS

Animal procedures

Animal procedures were approved and supervised by the local authorities and carried out in accordance with international and national guidelines. Twenty adult male C57/B6 mice (Charles River, Sulzfeld, Germany), weighing 20–25 g, were used for the experiments. Animals were randomly divided into four groups and exposed to 60 min of transient focal ischemia, applying the widely used left hemispheric thread occlusion model (MCAO). Animals were investigated on days 3, 7, 14 and 28 ($n = 5$ per group) and sacrificed directly after MRE acquisition. After aortic arch perfusion, brains were removed and indirectly frozen with fluid nitrogen.

MRE – mechanical stimulation

Mouse brains were mechanically stimulated as illustrated in ref. (14). Briefly, the vibration source was an electromagnetic coil attached to a carbon fiber piston, the end of which was mounted to the respiratory mask with a bite-bar transducer (Fig. 1a). The transducer was gimballed through a rubber bearing and retaining bracket at the temperature-controlled mouse bed.

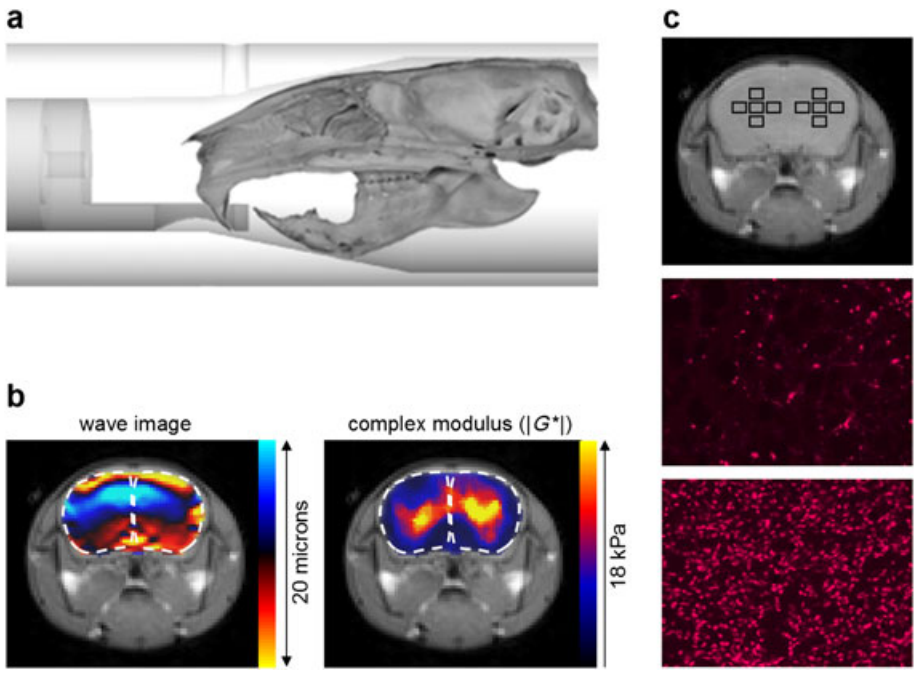

Figure 1. Experimental set-up and micrographs of immunohistochemically stained neurons. (a) Cut-out of the excitation device showing a mouse skull hooked to the bite bar. (b) Representations of shear waves and complex shear modulus in the mouse brain (color scales) overlaid with anatomic information obtained by T_1-weighted MRI (gray scale). Regions of interest used for MRE, comprising the visible brain parenchyma of the left and right hemispheres, were assigned on the basis of T_1-weighted MRI (white broken lines). (c) Regions of interest for the neuron counts (open boxes in the gray-scale image) and appearance of neuronal cell bodies with immunohistochemical staining. The number of neurons counted in the micrographs was reduced significantly in the stroke region (top) relative to the contralateral side (bottom). (For further details, please see the Methods section.)

The entire set-up was held in the center of the magnet bore by a plastic disk. Vibrations were produced by applying a sinusoidal current with a frequency of 900 Hz to an air-cooled Lorentz coil in the fringe field of the MRI scanner. The frequency amplitude and number of sinusoidal oscillation cycles were controlled by an arbitrary function generator connected via an audio amplifier to the driving coil. The main polarization of the vibration was transverse to the axis of the main magnetic field, with amplitudes on the order of tens of micrometers.

MRE – data acquisition

As described previously (33), all measurements were performed on a 7-T scanner (Bruker PharmaScan 70/16, Ettlingen, Germany) running ParaVision 4.0 software and using a 20-mm-diameter mouse head coil. The vibration was initiated by a trigger pulse from the control unit of the scanner, the timing of which was defined by a customized fast low-angle shot (FLASH) sequence. The pulse sequence was modified for MRE by a sinusoidal motion-sensitizing gradient (MSG) in the through-plane direction, as described in ref. (33). The MSG strength was 285 mT/m with a frequency of 900 Hz and nine periods. To compensate for static phase contributions, phase-difference images were calculated from two images differing in the sign of the MSG. Further imaging parameters were as follows: matrix, 128×128; field of view (FOV), 25 mm; TE = 14.3 ms; TR = 116.2 ms; eight dynamic scans over a vibration period; one transverse 2-mm slice centered to the bregma; acquisition time, 20 min.

MRE – data analysis

Complex wave images corresponding to the harmonic drive frequency were calculated by temporal Fourier transformation of the unfolded phase-difference images, and were filtered to suppress noise and compression wave components using a spatiotemporal Butterworth bandpass with cut-off frequencies of 0.6 and 1.24 mm (11,14). The preprocessed two-dimensional scalar wave fields were analyzed for the complex shear modulus G^* by planar algebraic Helmholtz inversion (34). Then, G^* was spatially averaged over two regions of interest (ROIs) corresponding to the left and right hemispheres displayed on the transverse image slice, and manually segmented by delineating its anatomical structure from MRE magnitude images (Fig. 1b). The average size of the ROIs in the left hemisphere was 10.4 ± 2.0 mm^2, and 10.3 ± 2.1 mm^2 in the right hemisphere (no statistically significant difference). The tabulated spatially averaged G^* values are represented by the real part of G^*, $G' = \mathrm{Re}(G^*)$, known as the storage modulus, the imaginary part $G'' = \mathrm{Im}(G^*)$, which is the loss modulus, the magnitude $|G^*| = \mathrm{abs}(G^*)$ and the loss tangent given by $\phi = \arctan(G''/G')$. The storage, loss and magnitude moduli are expressed in kilopascals (kPa), whereas ϕ is given in radians.

Histology

Sections were cut from brains, and immunohistochemical stainings were carried out to assess neuronal loss using NeuN (anti-NeuN antibody; Millipore, Schwalbach, Germany) and GFAP (anti-GFAP antibody; Abcam, Cambridge, UK) for astrocyte staining. Apoptosis was visualized using an ApopTag Red Kit (Millipore).

Cell counts were carried out in brain slices 0.5 mm posterior to the bregma within the region analyzed by MRE; NeuN was performed in five representative ROIs of 0.2 mm^2 for each hemisphere (Fig. 1c).

Statistical analysis

One-way analysis of variance (ANOVA) was used to test the influence of time on the MRE parameters and the histological parameters. A Wilcoxon signed-rank test was performed for pairwise comparison between hemispheres, and Pearson's correlation coefficient was calculated for cross-parameter evaluation. All analyses were conducted using SPSS Statistics 19 for Windows with the level of significance set at 0.05.

RESULTS

Figure 2 illustrates the histological findings in the left and right hemispheres of five mice on 4 days after transient MCAO, which, in the following, are labeled '_left' and '_right', respectively. ANOVA revealed no influence of time on NeuN, but there was a significant decrease in ApopTag_left (p 0.001). Transient increases in GFAP_left ($p < 0.001$) and GFAP_right ($p = 0.002$) were determined until day 7, followed by subsequent decays until day 28, which is the last time point at which measurements were performed in this study. Interhemispheric differences were significant for all markers on each day of measurement ($p < 0.001$). In agreement with the literature, NeuN_left was reduced relative to the contralateral marker, whereas GFAP_left and ApopTag_left were higher than the control side, although no apoptosis was appreciable in the right hemisphere (35,36).

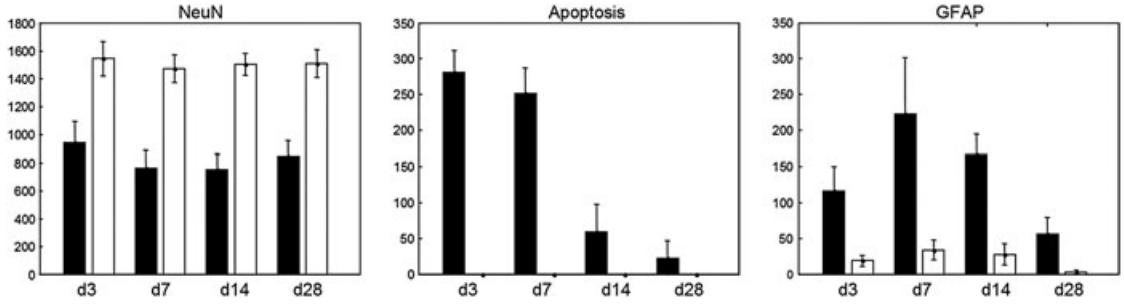

Figure 2. Histological markers on days 4, 7, 14 and 28 after transient middle cerebral artery occlusion (MCAO). Black bars refer to the ischemic territory, and white bars denote the contralateral region. All interhemispheric differences are significant with $p < 0.001$. NeuN did not change over time. GFAP, glial fibrillary acidic protein; NeuN, neuron count.

NMR IN BIOMEDICINE

Similar to NeuN, the MRE constants shown in Figure 3 were not significantly influenced by time. Henceforth, we combined all groups and further analyzed the time-constant complex shear modulus. In the combined group of 20 mice, G' and abs(G^*) proved that the brain elasticity was reduced in the stroke region relative to the control hemisphere (G'_left = 6.2 ± 1.8 *versus* G'_right = 6.9 ± 1.8 kPa, $p = 0.033$), whereas G'' and ϕ were not sensitive to MCAO.

Figure 4 displays the correlation between the complex shear modulus parameters and NeuN. For G'_left, G''_left and absG^*_left, Pearson's correlation coefficients were $R = 0.65$, 0.76 and 0.67, respectively (all $p < 0.005$), whereas there was no correlation between ϕ and NeuN_left. The relative variation of NeuN_left among all mice was 17%, compared with only 6% for NeuN_right, indicating the heterogeneity of the pathophysiological responses to transient MCAO in our group. As a result of the lower variability of NeuN_right relative to NeuN_left, we observed lower correlation coefficients with values of $R = 0.62$, 0.20 and 0.55 for G'_right, G''_right and absG^*_right, which, in this case, were significant only for G'_right ($p = 0.003$) and absG^*_right ($p = 0.013$). For the analysis of whole-brain effects, we averaged G', G'' and absG^* within both regions of the left and right hemispheres, and tested their correlations with NeuN = NeuN_left + NeuN_right. The correlation coefficients obtained were in the same order as observed for the left hemisphere ($R = 0.68$, 0.54, 0.64 and $p = 0.001$, 0.014, 0.002, respectively), which further indicates the sensitivity of MRE to the neuronal density. There was no correlation between any MRE parameter and GFAP or ApopTag. The averages of all parameters are summarized in Table 1.

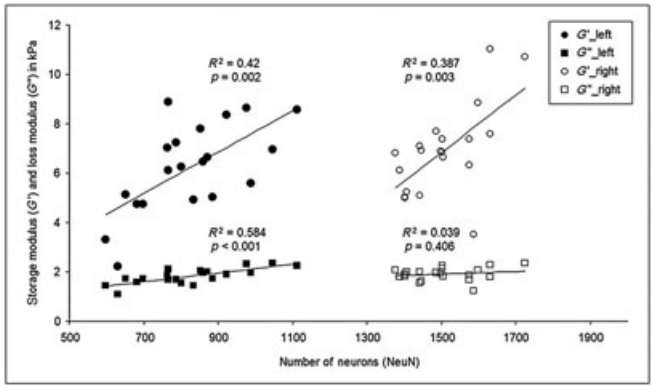

Figure 4. Correlation of MR elastography (MRE) parameters with the number of neurons in the mouse brain after middle cerebral artery occlusion (MCAO) of the left hemisphere. Regression lines refer to a linear correlation analysis, the responses of which (given by Pearson's correlation coefficients R and p values) are also shown.

DISCUSSION

The measurement of the mechanical constants of the brain for diagnostic purposes is an active area of research (37). Most cerebral MRE studies in the literature have focused on diffuse patterns of elasticity changes associated with various neurological disorders, such as MS, NPH or AD (23,25,27). Cerebral infarction in humans was addressed by a preliminary MRE study, which found softening within an extended ischemic territory 4 days after ischemic injury (5). Martín *et al.* (6) used ultrasound-based SWI to analyze the effect of MCAO on shear elasticity in rat brains.

In principle, MRE and SWI provide similar information about the shear modulus of soft tissue; however, the two methods differ in the way in which the mechanical excitation is achieved and in the algorithm used for wave analysis. MRE is based on time-harmonic shear waves induced by an external source, i.e. steady-state waves propagating from outside the body into the brain are captured in synchrony with image acquisition. In contrast, SWI relies on transient (shock) waves created by an internal source of focused ultrasound impulses, whose propagation

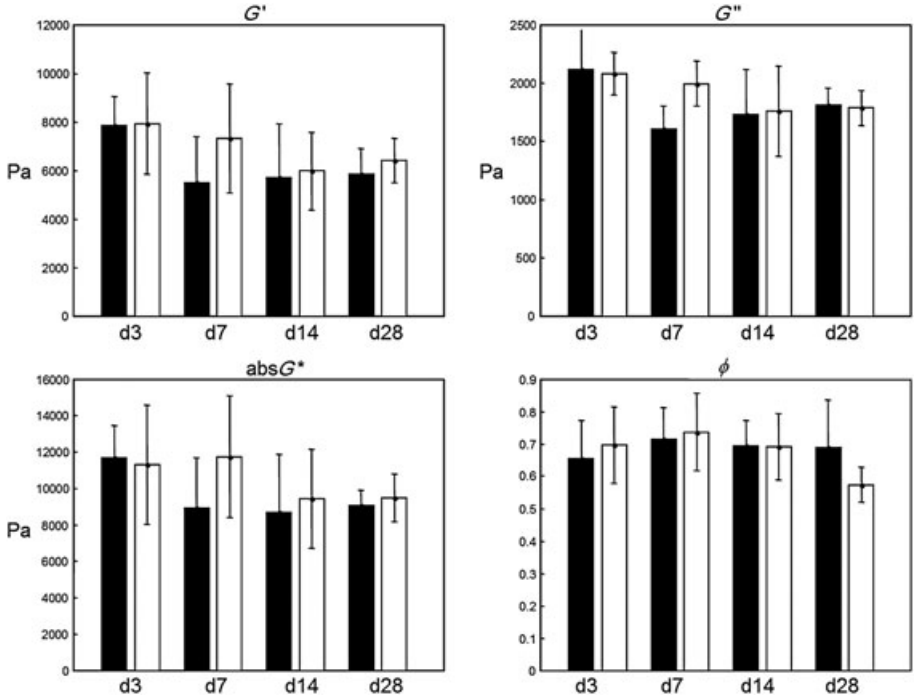

Figure 3. MR elastography (MRE) parameters on days 4, 7, 14 and 28 after transient middle cerebral artery occlusion (MCAO).

Table 1. Group-averaged parameters of MR elastography (MRE) and histology determined in 20 mice

	G' (Pa)	G'' (Pa)	absG^* (Pa)	ϕ (rad)	NeuN	GFAP	ApopTag
Mean_left	6219	1815	9576	0.687	825	140	153
SD_left	1752	316	2402	0.104	139	76	121
Mean_right	6901	1904	10494	0.674	1506	21	0
SD_right	1770	260	2700	0.110	97	16	0
p (left–right)	0.033	0.332	0.048	0.601	<0.001	<0.001	<0.001

absG^*, magnitude of the complex shear modulus; ApopTag, apoptosis; G', storage modulus; G'', loss modulus; GFAP, glial fibrillary acidic protein; NeuN, neuron count; SD, standard deviation; '_left' and '_right', left (ischemic) and right (control) hemispheres, respectively.

speed is analyzed by a time-of-flight algorithm (7). Such analysis of transient waves potentially alleviates the imposition of boundary effects, which are present in the solution of the time-harmonic inverse problem of single-frequency MRE, and limit the spatial resolution of elastograms generated with this technique. However, as time-harmonic waves in the low audible frequency range can penetrate deep into the body, MRE is currently the only noninvasive method of measurement of viscoelastic parameters in the brain.

Therefore, our study differs significantly from previous work in that it provides, for the first time, an elastographic view into the ischemic murine brain without removal of parts of the skull. Sustaining normal intracranial pressure and brain perfusion within the unopened skull may be critical to viscoelastic parameters, as has been indicated by MRE in rats (9) and invasive mechanical tests in porcine brain (38). Developments to improve the spatial resolution of MRE are underway (39–41).

So far, in our pilot study, we have focused on spatially averaged mechanical parameters based on regions referring to the dimensions of the left and right hemispheres. Of note, the evaluated MRE regions are larger than the ischemic territory and the corresponding contralateral region analyzed by histology. It is therefore not surprising that G' and absG^* are sensitive to MCAO only when the groups are considered together, whereas histological markers are altered significantly at each point in time following ischemic injury. Furthermore, transient MCAO stimulates angiogenesis in the whole brain, including contralateral nonischemic areas (6,42). Considering the poroelastic properties of soft biological tissues, such changes in the solid–fluid fraction of the tissue would certainly influence our MRE values of *both* hemispheres (43). At any rate, the influence of perfusion pressure and vasculature on the mechanical properties of the brain is widely unexplored and requires further investigation. The literature reports increased cerebral shear moduli in rats immediately after death, which suggests that shear elastic properties are sensitive to altered perfusion and blood flow conditions in the brain (9). However, the sensitivity of MRE to pressure and poroelastic effects is expected to decrease with increasing dynamics (29,30), whereas, under transient dynamic conditions, as in SWI, no correlation between hyperperfusion and stiffness was observed (6). It remains to be determined by multifrequency MRE at which dynamic range cerebral perfusion can alter significantly the measured shear elastic properties. Furthermore, a multifrequency evaluation of the dispersion of the complex shear modulus would allow us to derive model-based viscoelastic constants which would provide insight into the alteration of the mechanical network hierarchy (33).

In general, multiple MCAO-related events and structural reorganization processes potentially affect the complex shear modulus measured by MRE. In brief, such processes may include:

- the disruption of neuronal integrity towards the loss of neurons and decreasing neuronal density;
- destruction of the extracellular matrix;
- necrotic liquefaction;
- an edematous increase in the amount of interstitial water;
- increased vessel density;
- inflammation and subsequent vascular and periventricular tissue alteration.

Our study addresses the influence of neuronal decline, necrosis and scarring on the macroscopic mechanical properties of the brain. The observed correlations between MRE values (G', G'', absG^*) and NeuN strongly suggest that the neuronal network contributes to the mechanical scaffold of the brain. Conversely, a constant phase angle ϕ would suggest an unaltered geometry of the network, even though single network elements are degraded as a result of transient MCAO. However, compared with previous work on multifrequency MRE in humans (18), the precision of the phase angle of the complex modulus is limited, which prevents us from drawing further conclusions about the sensitivity of cerebral MRE to neuronal network structures.

Beyond neuronal cell loss as a result of necrosis and secondary apoptotic cell death, we measured an increased number of GFAP-positive astrocytes within the ischemic core. During the short observation period in our study, reactive astrocytes and glial scar formation appeared to have a minor influence on the measured mechanical constants, and may thus be counteracted by the overall loss of cells in the affected hemisphere and a possibly lower degree of tissue organization (44).

In summary, we altered the cerebral tissue structure in the mouse by transient MCAO. MRE was used to measure the *in vivo* complex shear modulus of the ischemic hemisphere in 20 mice on days 3, 7, 14 and 28 after 1 h of MCAO, and to compare the values of the storage modulus, loss modulus, magnitude modulus and phase angle of the complex modulus with values obtained in the contralateral hemisphere. Furthermore, the correlation of the MRE parameters with histological markers was tested. Our results corroborate findings from the literature that ischemic cerebral tissue is softer than healthy tissue. Furthermore, a significant correlation between the shear modulus of brain tissue and NeuN was observed. This correlation was stronger in the ischemic hemisphere than in healthy tissue, where the variability in NeuN between animals was less pronounced than in the infarcted region.

Acknowledgement

Financial support of the German Research Foundation (Br 2235/3 and Sa 901/4) is gratefully acknowledged.

REFERENCES

1. Plate KH. Mechanisms of angiogenesis in the brain. J. Neuropathol. Exp. Neurol. 1999; 58: 313–320.
2. Lin CY, Chang C, Cheung WM, Lin MH, Chen JJ, Hsu CY, Chen JH, Lin TN. Dynamic changes in vascular permeability, cerebral blood volume, vascular density, and size after transient focal cerebral ischemia in rats: evaluation with contrast-enhanced magnetic resonance imaging. J. Cereb. Blood Flow Metab. 2008; 28: 1491–1501.
3. Brea D, Sobrino T, Ramos-Cabrer P, Castillo J. Inflammatory and neuroimmunomodulatory changes in acute cerebral ischemia. Cerebrovasc. Dis. 2009; 27(Suppl. 1): 48–64.
4. Thiel A, Heiss WD. Imaging of microglia activation in stroke. Stroke 2011; 42: 507–512.
5. Hirsch S, Streitberger KJ, Hoffmann JR, Klingebiel R, Klatt D, Papazoglou S, Braun J, Sack I. MR elastography of stroke: a feasibility study. *Proceedings of the 18th Annual Meeting ISMRM*, Stockholm, Sweden, 2011; 1072.
6. Martín A, Macé E, Boisgard R, Montaldo G, Thézé B, Tanter M, Tavitian B. Imaging of perfusion, angiogenesis, and tissue elasticity after stroke. J. Cereb. Blood Flow Metab. 2012; 32: 1496–1507.
7. Bercoff J, Pernot M, Tanter M, Fink M. Monitoring thermally-induced lesions with supersonic shear imaging. Ultrason. Imaging 2004; 26: 71–84.
8. Muthupillai R, Ehman RL. Magnetic resonance elastography. Nat. Med. 1996; 2: 601–603.
9. Vappou J, Breton E, Choquet P, Willinger R, Constantinesco A. Assessment of in vivo and post-mortem mechanical behavior of brain tissue using magnetic resonance elastography. J. Biomech. 2008; 41: 2954–2959.
10. Atay SM, Kroenke CD, Sabet A, Bayly PV. Measurement of the dynamic shear modulus of mouse brain tissue in vivo by magnetic resonance elastography. J. Biomech. Eng. 2008; 130: 021013.
11. Clayton EH, Garbow JR, Bayly PV. Frequency-dependent viscoelastic parameters of mouse brain tissue estimated by MR elastography. Phys. Med. Biol. 2011; 56: 2391–2406.
12. Murphy MC, Curran GL, Glaser KJ, Rossman PJ, Huston J 3rd, Poduslo JF, Jack CR Jr, Felmlee JP, Ehman RL. Magnetic resonance elastography of the brain in a mouse model of Alzheimer's disease: initial results. Magn. Reson. Imaging, 2011; 30: 535–539.
13. Schregel K, Wuerfel E, Garteiser P, Gemeinhardt I, Prozorovski T, Aktas O, Merz H, Petersen D, Wuerfel J, Sinkus R. Demyelination reduces brain parenchymal stiffness quantified in vivo by magnetic resonance elastography. Proc. Natl. Acad. Sci. USA 2012; 109: 6650–6655.
14. Riek K, Millward JM, Hamann I, Mueller S, Pfueller CF, Paul F, Braun J, Infante-Duarte C, Sack I. Magnetic resonance elastography reveals altered brain viscoelasticity in experimental autoimmune encephalomyelitis. NeuroImage Clin. 2012; 1: 81–90.
15. Kruse SA, Rose GH, Glaser KJ, Manduca A, Felmlee JP, Jack CR Jr, Ehman RL. Magnetic resonance elastography of the brain. Neuroimage 2008; 39: 231–237.
16. Sack I, Beierbach B, Hamhaber U, Klatt D, Braun J. Non-invasive measurement of brain viscoelasticity using magnetic resonance elastography. NMR Biomed. 2008; 21: 265–271.
17. Green MA, Bilston LE, Sinkus R. In vivo brain viscoelastic properties measured by magnetic resonance elastography. NMR Biomed. 2008; 21: 755–764.
18. Sack I, Beierbach B, Wuerfel J, Klatt D, Hamhaber U, Papazoglou S, Martus P, Braun J. The impact of aging and gender on brain viscoelasticity. Neuroimage 2009; 46: 652–657.
19. Sack I, Streitberger KJ, Krefting D, Paul F, Braun J. The influence of physiological aging and atrophy on brain viscoelastic properties in humans. PlosOne 2011; 6: e23451.
20. Zhang J, Green MA, Sinkus R, Bilston LE. Viscoelastic properties of human cerebellum using magnetic resonance elastography. J. Biomech. 2011; 44: 1909–1913.
21. Johnson CL, McGarry MD, Van Houten EE, Weaver JB, Paulsen KD, Sutton BP, Georgiadis JG. Magnetic resonance elastography of the brain using multishot spiral readouts with self-navigated motion correction. Magn. Reson. Med. 2012; doi: 10.1002/mrm.24473. [Epub ahead of print].
22. Clayton EH, Genin GM, Bayly PV. Transmission, attenuation and reflection of shear waves in the human brain. J. R. Soc. Interface 2012; 9: 2899–2910.
23. Wuerfel J, Paul F, Beierbach B, Hamhaber U, Klatt D, Papazoglou S, Zipp F, Martus P, Braun J, Sack I. MR-elastography reveals degradation of tissue integrity in multiple sclerosis. Neuroimage 2010; 49: 2520–2525.
24. Streitberger KJ, Sack I, Krefting D, Pfüller C, Braun J, Paul F, Wuerfel J. Brain viscoelasticity alteration in chronic-progressive multiple sclerosis. PlosOne 2012; 7: e29888.
25. Murphy MC, Huston J 3rd, Jack CR Jr, Glaser KJ, Manduca A, Felmlee JP, Ehman RL. Decreased brain stiffness in Alzheimer's disease determined by magnetic resonance elastography. J. Magn. Reson. Imaging 2011; 34: 494–498.
26. Murphy MC, Huston J 3rd, Glaser KJ, Manduca A, Meyer FB, Lanzino G, Morris JM, Felmlee JP, Ehman RL. Preoperative assessment of meningioma stiffness using magnetic resonance elastography. J. Neurosurg. 2013; 118: 643-648.
27. Streitberger KJ, Wiener E, Hoffmann J, Freimann FB, Klatt D, Braun J, Lin K, McLaughlin J, Sprung C, Klingebiel R, Sack I. In vivo viscoelastic properties of the brain in normal pressure hydrocephalus. NMR Biomed. 2011; 24: 385–392.
28. Freimann FB, Streitberger KJ, Klatt D, Lin K, McLaughlin J, Braun J, Sprung C, Sack I. Alteration of brain viscoelasticity after shunt treatment in normal pressure hydrocephalus. Neuroradiology 2012; 54: 189–196.
29. Weaver JB, Pattison AJ, McGarry MD, Perreard IM, Swienckowski JG, Eskey CJ, Lollis SS, Paulsen KD. Brain mechanical property measurement using MRE with intrinsic activation. Phys. Med. Biol. 2012; 57: 7275–7287.
30. Hirsch S, Klatt D, Freimann F, Scheel M, Braun J, Sack I. In vivo measurement of volumetric strain in the human brain induced by arterial pulsation and harmonic waves. Magn. Reson. Med. 2012; doi: 10.1002/mrm.24499. [Epub ahead of print].
31. Romano A, Scheel M, Hirsch S, Braun J, Sack I. In vivo waveguide elastography of white matter tracts in the human brain. Magn. Reson. Med. 2012; 68: 1410–1422.
32. Lu YB, Franze K, Seifert G, Steinhäuser C, Kirchhoff F, Wolburg H, Guck J, Janmey P, Wei EQ, Käs J, Reichenbach A. Viscoelastic properties of individual glial cells and neurons in the CNS. Proc. Natl. Acad. Sci. USA 2006; 103: 17 759–17 764.
33. Riek K, Klatt D, Nuzha H, Mueller S, Neumann U, Sack I, Braun J. Wide-range dynamic magnetic resonance elastography. J. Biomech. 2011; 44: 1380–1386.
34. Papazoglou S, Hamhaber U, Braun J, Sack I. Algebraic Helmholtz inversion in planar magnetic resonance elastography. Phys. Med. Biol. 2008; 53: 3147–3158.
35. Rupalla K, Allegrini PR, Sauer D, Wiessner C. Time course of microglia activation and apoptosis in various brain regions after permanent focal cerebral ischemia in mice. Acta Neuropathol 1998; 96: 172-178.
36. Barreto GE, Sun X, Xu L, Giffard RG. Astrocyte proliferation following stroke in the mouse depends on distance from the infarct. PlosOne 2001; 6: e27881.
37. Glaser KJ, Manduca A, Ehman RL. Review of MR elastography applications and recent developments. J. Magn. Reson. Imaging 2012; 36: 757–774.
38. Gefen A, Margulies SS. Are in vivo and in situ brain tissues mechanically similar? J. Biomech. 2004; 37: 1339–1352.
39. McLaughlin JR, Zhang N, Manduca A. Calculating tissue shear modulus and pressure by 2D Log-Elastographic methods. Inverse Probl. 2010; 26: 085007.
40. Papazoglou S, Hirsch S, Braun J, Sack I. Multifrequency inversion in magnetic resonance elastography. Phys. Med. Biol. 2012; 57: 2329–2346.
41. McGarry MD, Van Houten EE, Johnson CL, Georgiadis JG, Sutton BP, Weaver JB, Paulsen KD. Multiresolution MR elastography using nonlinear inversion. Med. Phys. 2012; 39: 6388–6396.
42. Cheung WM, Chen SF, Nian GM, Lin TN. Induction of angiogenesis related genes in the contralateral cortex with a rat three-vessel occlusion model. Chin. J. Physiol. 2000; 43: 119–124.
43. Perrinez PR, Pattison AJ, Kennedy FE, Weaver JB, Paulsen KD. Contrast detection in fluid-saturated media with magnetic resonance poroelastography. Med. Phys. 2010; 37: 3518–3526.
44. Pekny M, Wilhelmsson U, Bogestål YR, Pekna M. The role of astrocytes and complement system in neural plasticity. Int. Rev. Neurobiol. 2007; 82: 95–111.